Photoelectron angular distributions in infrared one-photon and two-photon ionization of FEL-pumped Rydberg states of helium

S Mondal[1], H Fukuzawa[1,2], K Motomura[1], T Tachibana[1], K Nagaya[2,3], T Sakai[3], K Matsunami[3], S Yase[3], M Yao[3], S Wada[2,4] H Hayashita[4], N Saito[2,5], C Callegari[6], K C Prince[6,7], P O'Keeffe[8], P Bolognesi[8], L Avaldi[8], C Miron[9], M Nagasono[2], T Togashi[10], M Yabashi[2], K L Ishikawa[11], I P Sazhina[12], A K Kazansky[13,14,15], N M Kabachnik[1,12,14] and K Ueda[1,2]

[1] Institute of Multidisciplinary Research for Advanced Materials, Tohoku University, Sendai 980-8577, Japan

[2] RIKEN SPring-8 Center, Kouto 1-1-1, Sayo, Hyogo 679-5148, Japan

[3] Graduate School of Science, Kyoto University, Kyoto 606-8502, Japan

[4] Graduate School of Science, Hiroshima University, Higashi-Hiroshima 739-8526, Japan

[5] National Institute of Advanced Industrial Science and Technology, NMIJ, Tsukuba 305-8568, Japan

[6] Elettra-Sincrotrone Trieste, 34149 Basovizza, Trieste, Italy

[7] eChemistry Laboratory, Faculty of Life and Social Sciences, Swinburne University of Technology, Melbourne, Victoria 3122, Australia

[8] CNR-Instituto di Metodologie Inorganiche e dei Plasmi, Area della Ricerca di Roma 1, 00015 Monterotondo, Italy

[9] Synchrotron SOLEIL, L'Orme des Merisiers, Saint-Aubin, BP 48, FR-91192 Gif-sur Yvette Cedex, France

[10] Japan Synchrotron Radiation Research Institute (JASRI), Kouto 1-1-1, Sayo, Hyogo 679-5198, Japan

[11] Photon Science Center, Graduate School of Engineering, The University of Tokyo, Tokyo 113-8656, Japan

[12] Skobeltsyn Institute of Nuclear Physics, Lomonosov Moscow State University, Moscow 119991, Russia

[13] Departamento de Fisica de Materiales, UPV/EHU, E-20018 San Sebastian/Donostia, Spain

[14] Donostia International Physics Center (DIPC), E-20018 San Sebastian/Donostia, Spain

[15] IKERBASQUE, Basque Foundation for Science, E-48011 Bilbao, Spain

E-mail: ueda@tagen.tohoku.ac.jp

Abstract. The photoelectron angular distributions (PADs) have been investigated for infrared (IR) ionization of He atoms excited to Rydberg states by extreme ultraviolet free-electron laser pulses. The experiment was carried out with two pulses which do not overlap in time. Depending on the intensity of the IR pulses, one IR photon ionization or additionally two-photon above-threshold ionization is observed. For low IR intensity the PAD is well described by a contribution of s and d partial waves in accordance with early experiments. At high IR intensity the PAD clearly shows the contribution of higher partial waves. The experimental data are compared with the results of theoretical calculations based on solving the time-dependent Schrödinger equation.

PACS numbers: 32.80.Rm, 32.80.Fb, 41.60.Cr

1. Introduction

Two-photon single ionization of He has attracted the attention of both experimentalists [1]–[14] and theoreticians [15]–[17] since this is the simplest non-linear process of photon interaction with the simplest two-electron atom, where all basic atomic properties are involved. In particular, if the extreme ultraviolet (EUV) photon has its energy below the ionization threshold of He, individual Rydberg states or a Rydberg-state manifold can be excited and further ionized by the second photon. In this case, according to the dipole selection rules, the outgoing electron can be described by a coherent superposition of s and d partial waves. The photoelectron angular distribution (PAD) is determined by the ratio of the moduli of the s and d amplitudes and the phase-shift difference between them. As has been demonstrated [8, 16], in this simple case, measurements of the PAD provide sufficient information to extract both the ratio and the phase-shift difference of the amplitudes, i.e. to obtain complete information about the two-photon ionization (TPI) process. Thus measurements of the PADs for TPI can serve as a stringent test for theoretical modeling.

Experimentally, the PADs in the TPI with excitation of Rydberg states have been measured using different EUV sources. In ref. [8] the EUV radiation from a high-order harmonic source was used to excite and align He atoms in 1snp ^{1}P states ($n = 3, 4$) with further ionization by an infrared (IR) laser field. From the measured PADs the ratio of transition amplitudes and the phase-shift difference $\delta_{\rm sd} = \delta_0 - \delta_2$ have been determined. Here δ_0 and δ_2 are the full phases of the s and d amplitudes. In particular, it was shown that the experimental $\delta_{\rm sd}$ agrees very well with the difference of the full electron scattering phase-shifts (which include the Coulomb phase-shifts) calculated by different methods for both s and d waves scattered off a He(1s)$^+$ ion. In ref. [13] the Rydberg 1snp states with $n = 4, 5$ and 6 were excited by synchrotron radiation and ionized by a synchronized IR pulsed laser. The obtained ratio of matrix elements and the phase-shift difference agree well with the measurements [8] and with the theoretical calculations.

In our recent work the single color TPI of He atoms has been investigated using ultrashort pulses of EUV free electron laser (FEL) [14]. The PADs have been measured at several excitation energies, thus probing the excitation and ionization of various Rydberg states or a manifold of them. In contrast to the previous two-color investigations, it was shown that the values of the phase-shift difference deviate considerably from the scattering phase-shift difference, if one or more excited levels, especially the Rydberg manifold, are within the spectral range of the EUV pulse. The deviation was attributed to the co-presence of resonant and nonresonant path contributions in the TPI by femtosecond pulses. As theoretically predicted by Ishikawa and Ueda [16, 17], the PAD in TPI is very sensitive to the relative contribution of resonant and nonresonant paths of ionization. When either the resonant or nonresonant mechanism dominates, the phase-shift difference $\delta_{\rm sd}$ is close to the scattering phase-shift difference. However, when several Rydberg states or the Rydberg manifold are

excited by a femtosecond pulse, the resonant and nonresonant paths give comparable contributions and $\delta_{\rm sd}$ can differ considerably from the value expected from the scattering phase-shift difference. Behaviors of the phases similar to those predicted in [16, 17] may be expected also in two-color TPI of He, namely, the $\delta_{\rm sd}$ may deviate from the scattering phase-shift difference also in this case. The necessary condition for this to occur is, however, the overlap of the exciting EUV and ionizing IR pulses. If the pulses do not overlap, the contribution of the direct two-photon ionization is negligible and only the resonant path contributes. Therefore, the phase-shift difference $\delta_{\rm sd}$ should again coincide with the scattering phase-shift difference.

In this paper, we extend our investigation of TPI in He excited by a femtosecond FEL pulse to Rydberg states, to the case when ionization is produced by the IR photons from a synchronized strong IR laser. The long-lived Rydberg states, excited by the EUV pulse are ionized by a delayed IR pulse. In this experiment it is not possible to achieve the condition of complete overlap of the two pulses due to a large temporal jitter of the FEL pulses, which is much larger than the duration of the IR and FEL pulses. We show that at sufficiently low IR intensity, in contrast to the case of single-color (single-pulse) two-photon ionization, the phase-shift difference $\delta_{\rm sd}$ coincides with the scattering phase-shift difference, in agreement with previous experiments [8, 13]. In addition, we have investigated the dependence of the two-color ionization on the intensity of the IR field. We show that at large intensity not only one IR photon can be absorbed, but also two, leading to the three-photon process of above threshold ionization (ATI). The PADs in the three-photon ionization differ considerably from those in the two-photon ionization and contain contributions from higher angular momenta.

In the next section the setup and the main parameters of the experiment are described. In section 3 we discuss the experimental results for low and high intensity of the IR laser field. Section 4 is devoted to the simulations based on the numerical solution of the time-dependent Schrödinger equation (TDSE). A summary and conclusions are given in section 5.

2. Experiment

We performed the experiments using the SPring-8 Compact SASE Source (SCSS) test accelerator in Japan [18] and an IR laser in a pump-probe scheme combined with a velocity map imaging (VMI) spectrometer. The experimental setup is shown in figure 1. The photon energy of the EUV pulses provided by the SCSS FEL was set to 24.3 eV. The pulses had a duration of 30 fs [11] and a spectral width of 0.3 eV (FWHM) including a fluctuation of photon energy of 0.13 eV (FWHM) [19]. During the experiments the average pulse energy of the FEL was 1.4 μJ. The focusing system, with a focal length of 1 m, consisted of a pair of elliptical and cylindrical mirrors coated with SiC [20]. The reflectivity of each mirror was 70 %. At the interaction region the diameter of the FEL beam was $\sim 15\mu$m (FWHM). IR pulses of wavelength 800 nm were generated by a Ti:sapphire laser with a chirped pulse amplification system and electronically

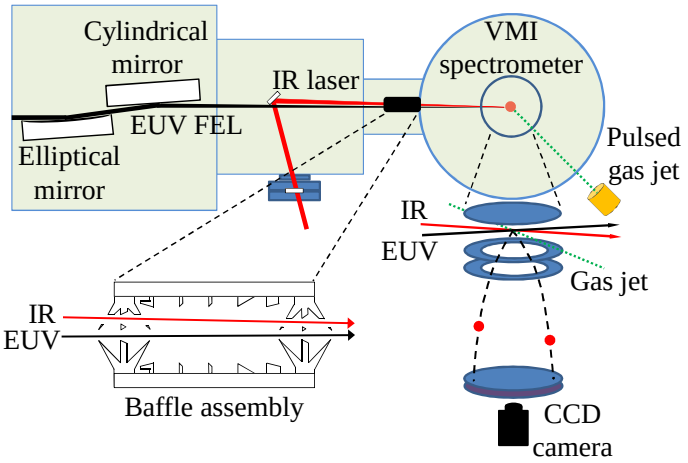

Figure 1. Schematics of the experimental setup. Inset: baffle assembly (see text for further details).

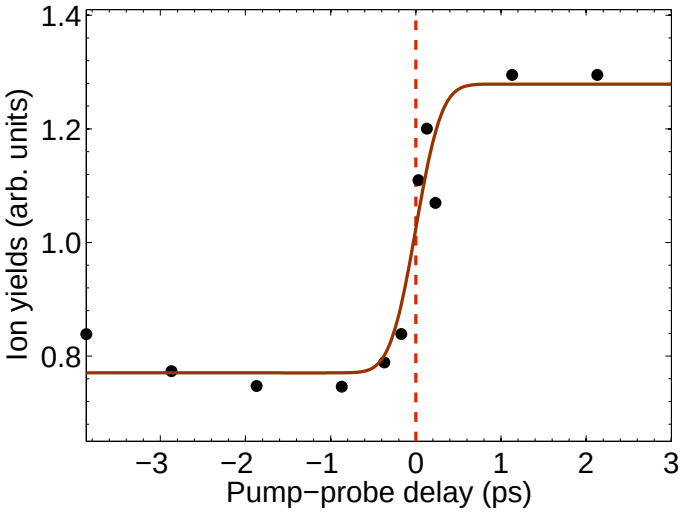

Figure 2. Helium ion yield as a function of the delay of IR pulses relative to the EUV pulses. The width of the step in the ion yield versus delay time gives the short term temporal jitter. See text for further details.

synchronized to the SCSS FEL pulses. The duration of the IR pulses was 30 fs [21]. The maximal IR laser pulse power was 0.63 mJ at the interaction region, and we attenuated the IR laser pulses by a neutral density filter in order to measure photoelectron spectra for different IR intensities. Before entering the experimental chamber, both EUV FEL and IR beams passed through a specifically designed baffle assembly, as illustrated in the inset of figure 1. This assembly successfully removed the majority of the scattered EUV light specularly and non-specularly reflected by the two mirrors, without reducing the FEL photon flux.

The IR beam intersects the EUV FEL beam at an angle of $\sim 1°$. The linear polarization direction of the IR laser nearly coincides with that of EUV FEL and lies in

the horizontal plane parallel to the detector plane of the VMI spectrometer. To align the IR beam to overlap with the EUV beam, we have carried out the following procedure. First we aligned the experimental chamber so that the FEL beam goes through the interaction region of the VMI spectrometer by viewing the spot using a Ce:YAG crystal located downstream of the interaction region. Then we aligned the IR beam so that it also goes through the interaction region in a similar manner. The timing of the EUV and IR pulses was crudely adjusted electronically by monitoring the signals by a PIN photodiode. Fine spatial overlap of the two pulses was achieved in the following manner. First, we employ ion yields of xenon atoms by the individual EUV and IR beams. Using the VMI spectrometer in the spatial imaging mode and detecting the xenon ions, we image the positions of the EUV and IR beams. We then adjust the IR beam image position to overlap with the EUV beam image position. This procedure accomplishes the overlap within the imaging plane (say, X-Y plane) but does not assure the overlap in the Z direction perpendicular to this plane. To achieve the spatial overlap including the Z direction, we use the helium ion yields. The helium atoms are not ionized by a single photon of 24.3 eV but are excited to the Rydberg manifold. When the IR beam is overlapped with the EUV beam then the helium atom excited to the Rydberg manifold will be ionized. By setting the IR pulses to come later ($\sim$100 ps) than EUV pulses based on the crude timing adjustment described above and sweeping the IR beam along the Z direction while monitoring the helium ion yields, we can achieve complete three dimensional overlap of the EUV and IR beams. Finally, by sweeping electronically the time delay of the IR pulses relative to the EUV pulses we can find time zero as seen in Figure 2, which depicts the time delay dependence of the helium ion yields around time zero thus obtained. By analyzing the width of the step in the ion yield versus delay time, we can estimate the temporal jitter of the FEL pulses to be $\sim$ 500 fs. Because of this large temporal jitter of the FEL pulses, which is much larger than the duration of the IR and EUV pulses, it is not possible to make the two pulses overlap in time. Furthermore the time zero obtained above (figure 2) within the temporal jitter is stable only for a few minutes, for a short time measurement. The measurements described below were mostly performed for non-overlapping pulses when the IR pulse came 10 ps later than the EUV pulses, to assure that the IR pulse comes second. The measurements setting the delay to time zero resulted in practically the same results within experimental uncertainty.

The photoelectrons produced due to the combined action of EUV FEL and IR pulses had their angular distribution cylindrically symmetric along the EUV and IR polarization axes. They were accelerated through the VMI spectrometer perpendicularly to both the propagation direction and linear polarization axis of the pulses, towards a position sensitive micro channel plate (MCP) detector followed by a phosphor screen. The positions of the detected electrons were recorded using a gated CCD camera synchronized with the arrival time of EUV pulses. An electrical gate pulse of 200 ns was applied to the back of the MCP detector. The three dimensional photoelectron momentum distribution is retrieved from the measured two dimensional projection of momentum distribution using a mathematical procedure based on the Abel inversion

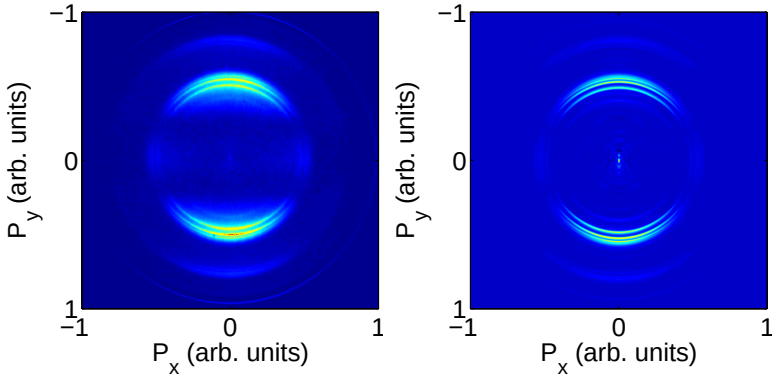

Figure 3. 2D projection (left) of the momentum distribution of the outgoing photoelectrons from IR dressed helium atoms irradiated by EUV FEL pulses at a photon energy of 24.3 eV, and the corresponding slice (right) through the retrieved 3D photoelectron momentum distribution as obtained from an Abel inversion.

[22], where the PAD was expressed in terms of Legendre polynomial expansion (up to the 10th order).

Figure 3 shows an example of raw and inverted images obtained when the IR laser pulse intensity was at its maximum (0.63 mJ). The inverted image in the figure corresponds to a slice through the cylindrically symmetric 3D velocity distribution of the ejected photoelectrons. The inverted image clearly shows several spectral maxima as concentric rings with a large radius corresponding to a large kinetic energy of the electrons. The energy resolution of the spectrometer is $\Delta E/E \approx 5\%$. Furthermore, the images show inner and outer groups of rings which correspond to the photoelectrons emitted due to ionization of helium by one and two IR photons, respectively, after excitation by a single EUV photon. The intensity distribution along the circumference of the rings defines the angular distribution of the photoelectrons. The advantage of the VMI spectrometer is that a complete angular distribution can be measured simultaneously with the photoelectron kinetic energy spectrum. In the case of three-photon (one EUV photon plus two IR photons) ionization processes, the PAD can be expressed by

$$I(\theta) = \frac{I_0}{4\pi}\left[1 + \beta_2 P_2(\cos\theta) + \beta_4 P_4(\cos\theta) + \beta_6 P_6(\cos\theta)\right] , \qquad (1)$$

where I_0 is the angle-integrated intensity and β_2, β_4 and β_6 are the anisotropy parameters associated with the second- fourth- and sixth-order Legendre polynomials $P_2(x)$, $P_4(x)$, and $P_6(x)$, respectively. The polar angle θ is the angle between the photoelectron velocity vector and the direction of the linear polarization of the EUV and IR photon beams. We note that $\beta_6 \equiv 0$ for two-photon (one EUV photon plus one IR photon) single ionization. The possible errors in obtaining these β values which may arise are due to inaccurate centering of the image and the selection of the number of pixels within the photoelectron peak. These factors are taken into account in the estimation of the overall error in experimentally measured β parameters.

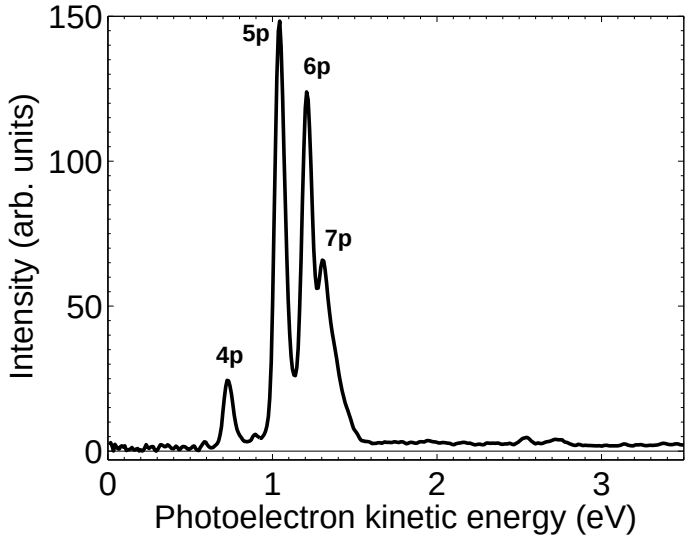

Figure 4. Photoelectron spectrum for TPI of He atoms irradiated by EUV FEL pulses at photon energy of 24.3 eV and dressed by the low-intensity IR pulse. The peaks are attributed to ionization of the corresponding Rydberg states excited by EUV pulses.

3. Experimental results

The spectra and angular distributions of photoelectrons have been measured at three different intensities of the IR laser pulse, corresponding to the laser pulse energies: 0.063 mJ, 0.11 mJ and 0.63 mJ. The spectrum obtained at the lowest intensity shows only peaks corresponding to one-IR-photon absorption from several Rydberg states with $n = 4 - 7$ (see figure 4). The states $n = 4 - 6$ are well resolved, while the states $n = 7$ and higher are not resolved. Analysis of the angular distributions made for each of the peaks gives β_2 and β_4 values which are presented in Table 1. Using these values we obtained the ratio of the s and d amplitudes $X = |A_s|/|A_d|$ and the phase-shift difference δ_{sd} as described in [16]. The ratio X and the phase-shift difference δ_{sd} agree well with experimental results by Haber *et al* [8] for the Rydberg states with $n = 3$ and 4 and by O'Keeffe *et al* [13] for the states with $n = 5$ and 6, as shown in figure 5. Theoretical calculations given in these papers [8, 13] are also shown in the figure. Our measurements, as well as other measurements agree well with these theoretical predictions. It should be noted that the theoretical phase-shift difference coincides with the scattering phase-shift difference that is intrinsic to the energy eigenfunction and thus is independent of the ionization pathway. Our experimental phase-shift difference for the unresolved Rydberg manifold with $n \geq 7$ also agrees well with the scattering phase-shift difference. This observation is in sharp contrast to the previous observation of EUV single-color TPI [14], where the phase-shift difference significantly deviated from the scattering phase-shift difference for the Rydberg manifold excitation.

When the IR field intensity increases, the second group of not completely resolved peaks appears in the spectrum which corresponds to the two-photon above-threshold

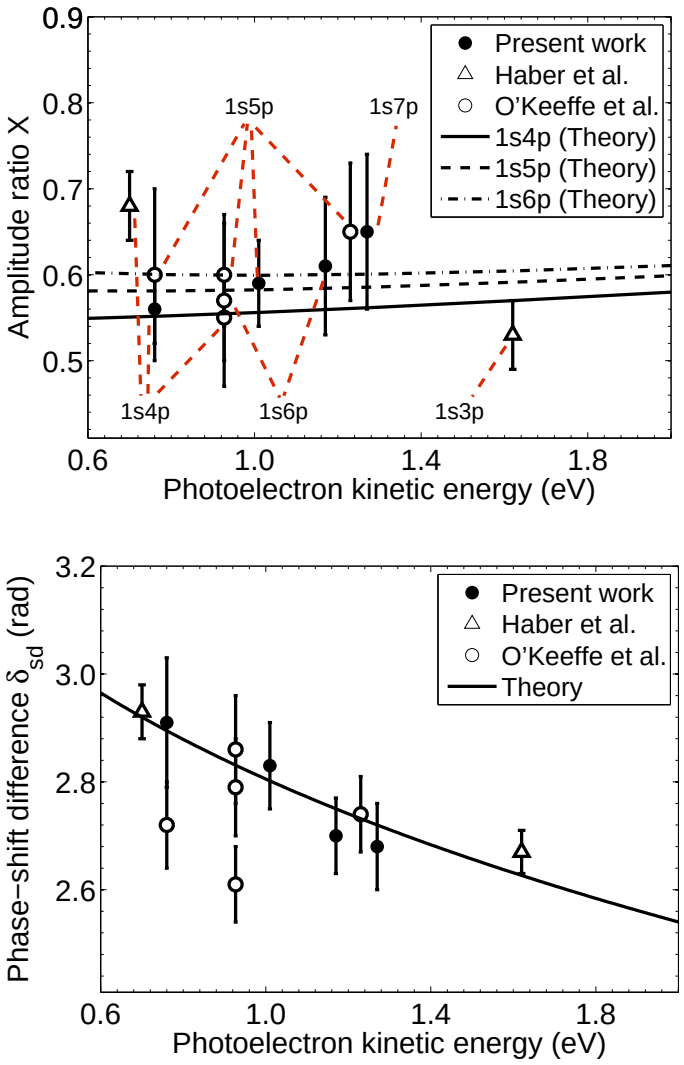

Figure 5. Amplitude ratio X (upper panel) and phase-shift difference $\delta_{\rm sd}$ (lower panel) as a function of photoelectron energy. Our results are compared with previous measurements [8, 13] and theoretical results presented in [13].

Table 1. Experimental values of asymmetry parameters β_2 and β_4 and derived phase-shift difference $\delta_{\rm sd}$ and amplitude ratios X for ionization of different Rydberg states as measured at the lowest IR intensity, corresponding to the laser pulse power 0.063 mJ.

State	E_e (eV)	β_2	β_4	$\delta_{\rm sd}$ (rad)	X
4p	0.76	2.94 ± 0.10	1.96 ± 0.04	2.91 ± 0.12	0.56 ± 0.04
5p	1.01	2.92 ± 0.07	1.91 ± 0.06	2.83 ± 0.08	0.59 ± 0.05
6p	1.17	2.84 ± 0.09	1.88 ± 0.09	2.70 ± 0.07	0.61 ± 0.08
7p	1.27	2.83 ± 0.11	1.81 ± 0.10	2.68 ± 0.08	0.65 ± 0.09

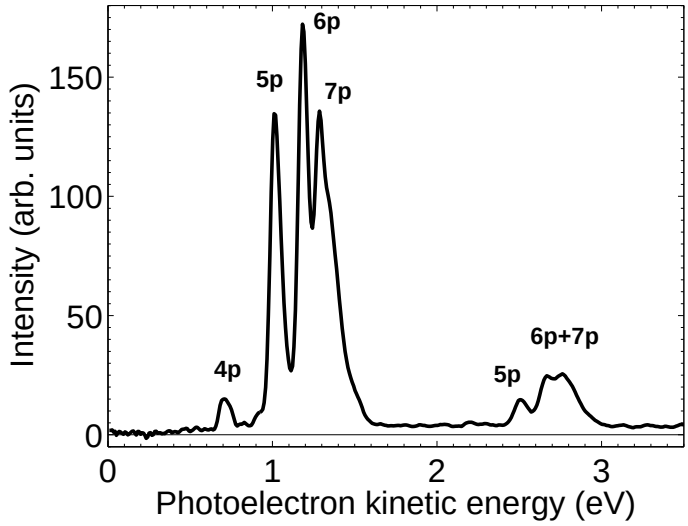

Figure 6. Photoelectron spectrum for IR ionization of He atoms irradiated by EUV FEL pulses at photon energy of 24.3 eV and dressed by the high-intensity IR pulse. The peaks are identified as one-IR-photon and two-IR-photon ionization of indicated Rydberg states excited by EUV pulses.

Table 2. Experimental and theoretical values of asymmetry parameters β_2, β_4 and β_6 for the three-photon ionization at the high intensity of the IR laser, corresponding to the laser pulse power 0.63 mJ.

State	E_e (eV)	Experiment			Calculation		
		β_2	β_4	β_6	β_2	β_4	β_6
5p	2.5	1.93 ± 0.08	1.49 ± 0.06	1.23 ± 0.13	2.24	1.9	1.11
6p+7p	2.8	2.39 ± 0.11	2.08 ± 0.10	1.77 ± 0.07	2.23	1.89	1.11

ionization of excited and aligned Rydberg states as seen in figure 6, which shows the photoelectron spectrum for the highest IR intensity (0.63 mJ). The PADs for this second maximum are notably narrower than for the first (one-photon) maximum (see figure 7). The angular distribution is described by three asymmetry parameters β_2, β_4 and β_6, which are presented in Table 2. Large β_6 asymmetry parameter clearly indicates that the PADs in the second maximum contain also contributions from higher partial waves. From the relative intensity of two-photon above-threshold ionization to the one-photon ionization of the excited Rydberg sates, we estimated also the effective intensity of the IR pulses to be 0.6×10^{12} W/cm^2. This value will be used in the calculations described in the next section.

4. Calculations

In order to elucidate further our observations, we have carried out numerical calculations solving the time-dependent Schrödinger equation (TDSE) in a single active electron

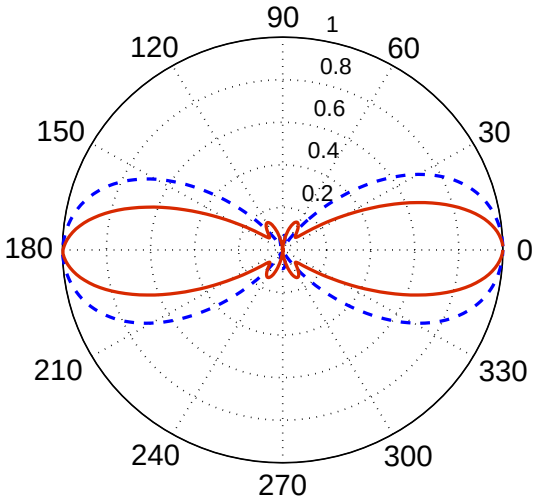

Figure 7. Comparison of polar plots of PADs for one-IR-photon ionization (blue dashed line) and two-IR-photon ionization (red solid line) from the $n = 5$ Rydberg state of He excited by EUV FEL pulses.

approximation. The details of the application of the TDSE to the problem of atomic ionization in the field of two EUV and IR pulses are given in earlier publications [23, 24]. In this work we use a slightly modified computer code which is adjusted to treat the low-energy electrons and the longer EUV and IR pulses. In order to make calculations feasible we considered shorter EUV pulses than in the experiment, namely with FWHM=7 fs, which is close to the coherence time of the FEL pulses [11], thus properly taking the experimental spectral width into account. The duration of the IR pulse was 30 fs. The calculations have been performed for the case of non-overlapping EUV and IR pulses, namely the time interval between the maximum of the EUV pulse and the beginning of the IR pulse was set equal to 500 a.u. (12.1 fs). For the envelope of the EUV and IR pulses we used the inverse hyperbolic cosine shape and cosine squared shape, respectively. For the description of the active electron in the ground state of He and in the continuum states we used the screened Coulomb potential with a polarization term:

$$v(r) = -\frac{2}{r} - \frac{1}{r}(e^{-4r} - 1) - 2e^{-4r} - \frac{9}{32}\frac{1}{(r^2 + 1.2)^2}. \qquad (2)$$

With this potential we reproduce the binding energy of the 1s electron in He quite accurately: the calculated value is 24.61 eV, the experimental value 24.59 eV [25]. Further details of the calculations can be found in references [23, 24].

At low IR intensity, the calculations with non-overlapping pulses reproduce well the observations (compare tables 1 and 3). Interestingly, when the two pulses temporarily overlap, the β_2 and β_4 parameters and therefore the phase-shift difference between the s and d waves deviate only slightly from the case of non-overlapping pulses (see table 3 for comparison). This is in contrast to similar calculations for two-color TPI of Ne and H, where a strong dependence of the asymmetry parameters on the time-delay is

Table 3. Comparison of the calculated values of asymmetry parameters β_2 and β_4 and the phase-shift difference $\delta_{\rm sd}$ at the photoelectron energy of 1.0 eV (5p Rydberg state ionization) for non-overlapping (a) and completely overlapping (b) EUV and IR pulses.

	β_2	β_4	$\delta_{\rm sd}$ (rad)
(a)	2.89	1.33	2.87
(b)	2.87	1.27	2.89

obtained [26]. It also differs from the case of the single-color single-pulse two photon ionization of He [14]. It seems, that the two-color TPI of the He atom indeed represents a special case in which the PAD barely varies with delay, accidentally, for the present combination of photon energies.

At high IR intensity, again TDSE calculations for non-overlapping pulses reproduce well the experimental results (see table 2) confirming the absence of nonresonant ionization paths and contributions from high-l partial waves to the PADs.

5. Conclusions

We have investigated experimentally and theoretically ionization by infrared laser pulses of He atoms excited by EUV FEL pulses in Rydberg states. The energy spectra and angular distribution of photoelectrons have been measured for different intensities of the IR pulses for the case when the EUV and IR pulses do not overlap in time. At low IR intensity our results agree with the previous measurements and theoretical predictions, confirming that in this case the extracted phase-shift difference between s and d partial waves coincides within experimental error with the value expected from the scattering phase-shift difference. At high IR intensity one-EUV-and-two-IR-photon ATI is observed. The PAD at the ATI peak differs considerably from that at the one-IR-photon peak showing a clear contribution of higher partial waves. The calculations based on the solution of the TDSE describe well the experimental results.

Acknowledgments

We are grateful to the SCSS Test Accelerator Operation Group at RIKEN for continuous support in the course of the studies and to the staff of the technical service section in IMRAM, Tohoku University, for their assistance in constructing the apparatus. This study was supported by the X-ray Free Electron Laser (XFEL) Utilization Research Project and the XFEL Priority Strategy Program of Ministry of Education, Culture, Sports, Science and Technology of Japan (MEXT), by the Management Expenses Grants for National Universities Corporations from MEXT, by Grants-in-Aid for Scientific Research from JSPS (No. 21244062 and No. 22740264), and IMRAM research program. SM would like to thank JSPS for financial support. NMK acknowledges

hospitality and financial support by IMRAM, Tohoku University (Sendai) and DIPC (Donostia/San Sebastian). KLI gratefully acknowledges support by the APSA Project (Japan), KAKENHI (No. 23656043 and No. 25286064), and the Cooperative Research Program of "Network Joint Research Center for Materials and Devices" (Japan).

References

[1] T. Sekikawa, A. Kosuge, T. Kanai, and S. Watanabe, *Nature* **432**, 605 (2004).
[2] N. Miyamoto, M. Kamei, D. Yoshitomi, T. Kanai, T. Sekikawa, T. Nakajima, and S. Watanabe, *Phys. Rev. Lett.* **93**, 083903 (2004).
[3] H. Hasegawa, E. J. Takahashi, Y. Nabekawa, K. L. Ishikawa, and K. Midorikawa, *Phys. Rev.* A **71**, 023407 (2005).
[4] O. Guyetand *et al., J. Phys. B: At. Mol. Opt. Phys.* **38**, L357 (2005).
[5] M. Meyer *et al., Phys. Rev.* A **74**, 011401(R) (2006).
[6] M. Meyer *et al., Phys. Rev. Lett.* **101**, 193002 (2008).
[7] O. Guyetand *et al., J. Phys. B: At. Mol. Opt. Phys.* **41**, 051002 (2008).
[8] L. H. Haber, B. Doughty, and S. R. Leone, *Phys. Rev.* A **79**, 031401(R) (2009).
[9] L. H. Haber, B. Doughty, and S. R. Leone, *Molecular Physics* **108**, 1241 (2010).
[10] L. H. Haber, B. Doughty, and S. R. Leone, *Phys. Rev.* A **84**, 013416 (2011).
[11] R. Moshammer *et al., Opt. Express* **19**, 21698 (2011).
[12] T. Sato *at al., J. Phys. B: At. Mol. Opt. Phys.* **44**, 161001 (2011).
[13] P. O'Keeffe, A. Mihelic, P. Bolognesi, M. Zitnik, A. Moise, R. Richte, and L. Avaldi, *New J. Phys.* **15**, 013023 (2013).
[14] R. Ma *et al., J. Phys. B: At. Mol. Opt. Phys.* **46**, accepted (2013).
[15] Nikolopoulos L A A and Lambropoulos P 2001 *J. Phys. B: At. Mol. Opt. Phys.* **34** 545
[16] K. L. Ishikawa and K. Ueda, *Phys. Rev. Lett.* **108** 033003 (2012).
[17] K. L. Ishikawa and K. Ueda, *Applied Sciences* **3**, 189 (2013).
[18] T. Shintake *et al., Nat. Photon.* **2**, 555 (2008).
[19] Y. Hikosaka *et al.*, *Phys. Rev. Lett.* **105**, 133001 (2010).
[20] H. Ohashi *et al., Nucl. Instrum. Methods* A **649**, 163 (2011).
[21] M. Yabashi *et al., J. Phys. B: At. Mol. Opt. Phys.* **46**, accepted.
[22] M. J. J. Vrakking, *Rev. Sci. Instrum.* **72**, 4084 (2001).
[23] A.K. Kazansky and N.M. Kabachnik, *J. Phys. B: At. Mol. Opt. Phys.* **40**, 2163 (2007).
[24] A.K. Kazansky and N.M. Kabachnik, *J. Phys. B: At. Mol. Opt. Phys.* **40** 3413 (2007).
[25] Ralchenko Yu, Kramida A E, Reader J and NIST ASD Team 2008 NIST Atomic Spectra Database (version 5.1.4) http://physics.nist.gov/asd3
[26] Mondal S 2013 to be published